Eur Biophys J (2015) 44:263–276
DOI 10.1007/s00249-015-1024-y

ORIGINAL PAPER

EBSA
Biophysics in Europe

Mechanisms of the self-assembly of EAK16-family peptides into fibrillar and globular structures: molecular dynamics simulations from nano- to micro-seconds

Soheila Emamyari[1] · Faezeh Kargar[1] · Vahid Sheikh-hasani[2] · Saeed Emadi[2] · Hossein Fazli[1,2]

Received: 19 November 2014 / Revised: 19 February 2015 / Accepted: 23 March 2015 / Published online: 2 April 2015

Abstract The self-assembly of EAK16-family peptides in a bulk solution was studied using a combination of all-atom and coarse-grained molecular dynamics simulations. In addition, specified concentrations of EAK16 peptides were induced to form fibrillary or globular assemblies in vitro. The results show that the combination of all-atom molecular dynamics simulations on the single- and double-chain levels and coarse-grained simulations on the many-chain level predicts the experimental observations reasonably well. At neutral pH conditions, EAK16-I and EAK16-II assemble into fibrillary structures, whereas EAK16-IV aggregates into globular assemblies. Mechanisms of the formation of fibrillar and globular assemblies are described using the simulation results.

Keywords Molecular self-assembly · EAK16 peptides · All-atom and coarse-grained MD simulation

Introduction

Peptides—short sequences of amino acids—serve as excellent building blocks in self-assembly phenomena because of their ease of their synthesis, small size, relative stability and chemical and biological modifiability (Colombo et al. 2007). Self-assembly of these molecules has attracted significant attention from scientists in various experimental and theoretical areas so far, and considerable effort has been made to understand this phenomenon (Aggeli et al. 2001; Vauthey et al. 2002; Hartgerink et al. 2002; Claussen et al. 2003; Kokkoli et al. 2006; Velichko et al. 2008; Valéry et al. 2011). The importance of peptide self-assembly is due to its relevance with a number of conformational diseases such as Alzheimer's disease, Parkinson's disease and type II diabetes on the one hand (Haass and Selkoe 2007; Roychaudhuri et al. 2009; Benilova et al. 2012; Bowerman and Nilsson 2012) and their potential for some applications such as drug delivery (Levine et al. 2013), antibody and protein delivery (Koutsopoulos et al. 2009; Koutsopoulos and Zhang 2012; Wen et al. 2013, 2014a), vaccine adjuvants (Rudra et al. 2010; Chen et al. 2013), surface engineering (Zhang et al. 1999) and scaffolding for tissue repair (Holmes 2002; Galler et al. 2008) on the other. In addition, self-assembly of macromolecules is an interesting phenomenon for scientists because of the rich basic science behind it.

Study of the self-assembly behavior of short peptides, which have similarities with biological peptides, is of great importance for understanding related phenomena such as fibril formation in Alzheimer's disease. One of the short peptides consisting of both charged and hydrophobic amino acids with noticeable similarities to fiber-forming biological peptides is EAK16. This peptide, which is an ionic complementary peptide, includes three types: EAK16-I, EAK16-II and EAK16-IV. The first discovered peptide of this family is EAK16-II, which is a small part of zuotin protein. Zhang (1992) and co-workers were the first group who reported the existence of zuotin protein in 1992. All three types of EAK16 peptide have 16 amino acids, including alanine (A), glutamic acid (E) and lysine (K), and the difference among the three types is in their amino acid

✉ Hossein Fazli
fazli@iasbs.ac.ir

[1] Department of Physics, Institute for Advanced Studies in Basic Sciences (IASBS), 45137-66731 Zanjan, Iran

[2] Department of Biological Sciences, Institute for Advanced Studies in Basic Sciences (IASBS), 45137-66731 Zanjan, Iran

arrangement, which causes their charge distributions to differ. Amino acid sequences of EAK16-I, EAK16-II and EAK16-IV are $(AEAK)_4$, $(AEAEAKAK)_2$ and AEAEAEAEAKAKAKAK, respectively. Accordingly, the charge distributions of EAK16-I, EAK16-II and EAK16-IV at neutral pH are $-+-+-+-+$, $--++--++$ and $----++++$, respectively. These peptides are amphiphilic. Each peptide can be oriented in such a way that the side chains of the E and K residues on one hand and side chains of the A residues on the other orient to opposite sides.

The self-assembly behavior of EAK16 peptides under different conditions in solutions has been studied experimentally (Hong et al. 2003, 2004, 2005; Jun et al. 2004; Yang et al. 2007a, b; Wang et al. 2008). In these studies, the effects of different factors that affect the molecular behavior of the peptides in the solution, such as ionic concentration, pH, incubation time and peptide concentration, have been investigated. It has been shown that at neutral pH, EAK16-I and EAK16-II peptides assemble into fibrillar structures, while EAK16-IV forms globular assemblies (Jun et al. 2004). Also, study of the self-assembly behaviors of EAK16-II and EAK16-IV peptides at different pH conditions has shown that EAK16-IV has a pH-dependent behavior unlike EAK16-II, whose self-assembly behavior is less sensitive to the pH value (Hong et al. 2003).

Experimental study of the self-assembly of peptides at the molecular level for understanding the nucleation mechanism and describing the kinetics of growth of the assemblies in early stages is not possible because of the small size of the peptides. Computer simulations play an increasingly important role in understanding the structural details and the mechanism of the self-assembly in biomolecular systems. Some simulation studies of EAK16 peptides have been performed. For example, all-atom simulation of a double-chain system of EAK16-II near a surface for analyzing the adsorption of the peptide to the surface and coarse-grained simulation of EAK16-IV peptide in the solution for studying its folding and dimerization have been performed (Yan et al. 2008; Sheng et al. 2010a, b). The effect of pH on the self-assembly behavior of the three types of EAK16 peptide in the presence of a hydrophobic surface has been studied using coarse-grained molecular dynamics simulations (Emamyari and Fazli 2014a). It has been shown that EAK16-I and EAK16-II peptides assemble into ribbon-like structures on the hydrophobic surface, regardless of the pH value; EAK16-IV assembles into ribbon-like structures at low and high pH ranges and forms disk-shaped assemblies on the hydrophobic surface at neutral pH. Also, the dependence of single-chain conformation and dimerization of the three types of EAK16 peptide on the pH of the solution has been studied using all-atom simulations, and it has been shown that the pH-dependent behaviors of EAK16-I and EAK16-II are very similar and differ considerably from that of EAK16-IV (Emamyari and Fazli 2014b).

The phenomena such as protein folding and self-assembly of peptides and proteins occur on large temporal and spatial scales, and study of them using computer simulations with atomistic resolution is very time consuming. Hence, to obtain relatively comprehensive information about these phenomena and the events that occur on the supermolecular levels, a combination of all-atom and coarse-grained simulations can be very useful (Izvekov and Voth 2005; Shi et al. 2006; Zhou et al. 2007; Peter and Kremer 2009). In such studies, small parts of the system are simulated on short timescales with atomistic details, and then the system on larger scales is simulated on longer timescales with reduced spatial resolution. Combination of computer simulations on different spatial and temporal scales has been widely used in the study of many macromolecular systems. For example, low resolution coarse-grained simulations have been combined with high-resolution all-atom ones to describe the complete processes of peptide aggregation and pore formation by alamethicin peptides in a hydrated lipid bilayer (Thøgersen et al. 2008). In another work, development of a coarse-grained model for molecular dynamics simulation of a hydrophobic dipeptide in aqueous solution was discussed (Villa et al. 2009). For the derivation of interaction functions between coarse-grained beads, a bottom-up strategy has been followed, and the potentials have been devised such that the resulting coarse-grained simulation reproduced the conformational sampling and the intermolecular interactions observed in an all-atom simulation of the same peptide.

It is known that fibrillation of peptides such as beta amyloid starts with the lag phase in which fibrils do not appear to a significant extent (Naiki et al. 1997; Serio et al. 2000; Uversky et al. 2002; Pedersen et al. 2004; Kayed et al. 2004). In the lag phase of the nucleation step, only oligomers (beta-sheet-rich species) are formed. Very little is known about the structure of amyloid protofibrils and the structure of the aggregates that precede fibril formation (Harper et al. 1997a, b; Walsh et al. 1997, 1999). It seems that study of the self-assembly of short peptides with similarities with amyloid peptide helps to shed some light on the less known lag phase of fibril formation.

In this article, we use a combination of all-atom and coarse-grained molecular dynamics simulations to study the self-assembly behavior of EAK16-I and EAK16-IV peptides. We use all-atom simulations to study the system on the single- and double-chain levels, and then we study many-chain systems using coarse-grained simulations. These simulations cover a temporal range from nano- to micro-seconds and help to understand the mechanism of the self-assembly of EAK16 peptides. Moreover, following Jun et al. (2004), we perform self-assembly experiments with EAK16-II and EAK16-IV. The main aim of our work is investigation of the

possibility of describing the experimental observations by a combination of simulations of various resolutions. We find that the combination of all-atom simulations of single- and double-chain systems and the coarse-grained simulation of many-chain system provides a valuable tool for predicting the experimental observations. The results of the simulations are in good agreement with our experimental observations and those reported in the literature. Our results show that on the single-chain level, intra-chain electrostatic interactions force EAK16-IV peptide to take a dominantly folded conformation with the hydrophobic side chains of the chain exposed to water. The same situation is observed to persist on the double-chain level, and the folded conformation of the two chains does not change considerably in the course of the dimerization process. Folding of EAK16-IV peptide in this manner causes it to aggregate into globular assemblies on the many-chain level. EAK16-I and EAK16-II chains, however, do not take a folded conformation because of weak intra-chain electrostatic interactions and their entropic tendency to have an extended conformation. All-atom simulations of a double-chain system of EAK16-I peptide show that a part of the two chains forms an antiparallel β-sheet. The β-sheets formed by pairs of EAK16-I peptide are observed to have the potential to stake over each other, forming fibrillar assemblies on the many-chain level. Formation of fibrillar assemblies by EAK16-I peptide chains, which happens by staking of β-sheets over each other and self-assembly of EAK16-IV chains into globular structures, is observed in our coarse-grained simulations.

Experimental materials and methods

Materials

We studied the aggregation behavior of EAK16-II and EAK16-IV peptides in solution experimentally using an atomic force microscope. As mentioned above, the molecular formula and weight of both peptides are the same: $C_{70}H_{121}N_{21}O_{25}$ and 1657, respectively. The peptides were purchased from Biomatik and used without further purification. The N- and C-terminal of the peptides are protected by acetyl and amino groups, respectively, to avoid electrostatic attractions between the ends of the peptide chains. Solutions of EAK16-II and EAK16-IV peptides were prepared at a concentration of 0.1 mg/ml, and the samples were stored at 4 °C before use. The experiments were performed at neutral pH.

Atomic force microscopy (AFM)

Nanostructures of peptide self-assemblies were observed using an AFM. To take AFM images, we put an amount of the solution on a freshly cleaved mica surface glued to a steel AFM sample plate. We left the sample for about 30 min (incubation time) to let the peptides stick to the mica surface. Then we washed the sample with about 100 μl of pure water to remove unattached peptides and left it for 3 h at room temperature to dry out completely. Then, we took the images using an AFM at room temperature in non-contact mode. A scanner with a maximum scan area of 5 × 5-μm^2 was used, and the resolution of images was 512 × 512 pixels.

All-atom and coarse-grained simulations: models and methods

All-atom simulations

All of the all-atom simulations were carried out using GROMACS package, version 4-0-7 (van der Spoel et al. 2005a, b; Hess et al. 2008) in the NPT ensemble. A dodecahedron simulation box with an edge length $l = 6$ nm was used. The volume of the simulation box was 152 nm^3. The box edge and box volume in double-chain simulations were 10 nm and 707 nm^3, respectively. The simulation box was filled with about 5000 (23000) single-point charge (SPC) water molecules in single- (double-) chain simulations (Berendsen et al. 1981). Lincs method was used to constrain all of the bond lengths to their equilibrium values, and the Settle algorithm was used to constrain water molecules (Hess et al. 1997; Miyamoto and Kollman 1992). Electrostatic interactions were calculated using the particle-mesh Ewald (PME) method with a cut-off distance of 1.0 nm (Darden et al. 1993; Essmann et al. 1995). The peptide and water molecules were coupled separately to a temperature bath at constant temperature, $T = 300°K$, with a coupling constant of 0.1 ps using the Berendsen algorithm. The pressure of the system was also kept in the same way at 1 bar with a coupling constant of 1 ps (Berendsen et al. 1984). Periodic boundary conditions were used in three dimensions in all of the simulations. Cut-off length, $\lambda_c = 1$ nm, was used for calculation of the Lennard-Jones interactions. The neighbor list was updated every ten steps, with a neighbor list cut-off distance of 1 nm. Before running the simulation of the system for each given set of parameters, we subjected it to a 3000-step steepest descent optimization to relax unfavorable contacts, followed by a 20-ps MD equilibration simulation with positional restraints on the peptide atoms using the leap-frog algorithm in an NPT ensemble (van Gunsteren and Berendsen 1988). The force constant on the peptide atoms in each direction (x, y and z) was 1000 kJ/(mol nm^2). After equilibration, full simulations were performed using an OPLS. AA all-atom force field with a time step of 2 fs (Jorgensen

and Tirado-Rives 1988). The VMD package was also used to visualize the conformation of the peptide chains (Humphrey et al. 1996). In an experimental study of the self-assembly phenomenon of the EAK16 peptide, the N (C)-terminal of the peptide chains was protected by an acetyl (amino) group to avoid end-to-end electrostatic attraction between the peptides. For the same purpose and regarding our available force fields, we used NH_2 and COOH groups instead of NH_3^+ and COO^- in the N- and C-terminal of the peptides to study them with no electric charges in their terminals (Emamyari and Fazli 2014b).

In the beginning of single chain simulation of each type, the peptide chain was in its extended conformation among water molecules. We produced the initial conformation of the peptide chain using HyperChem software [HyperChem (TM), Hypercube, Inc., USA]. We considered the time it takes the total energy of the system to reach a stable value as the system equilibration time. This time was found to be at most 10 ns. The values of the desired quantities were averaged over time after equilibration of the system. To probe the time evolution of the conformation of a peptide chain, we calculated its radius of gyration in the course of the simulation. We also calculated the time-averaged separation between the amino acids of each peptide chain after equilibration of the system. The separation between a pair of amino acids along a peptide chain was defined as the separation between their center of mass. In addition, snapshots of the system in the simulations were used for probing the conformational evolution of the peptide chains and for comparison with the quantitative results.

Coarse-grained simulations

The behavior of many-chain systems of EAK16-I and EAK16-IV peptides were studied using the MARTINI coarse-grained model (Marrink et al. 2007; Monticelli et al. 2008) and the GROMACS package, version 4-0-7 (van der Spoel et al. 2005a, b; Hess et al. 2008). In this model, the coordinates of all the atoms of the peptide chains and the secondary structure of the peptides should be known. To begin the simulation using this model, the secondary structure should first be assigned to the peptide chains. The secondary structure of the peptides remains fixed along the simulation (Marrink et al. 2007; Monticelli et al. 2008). The coordinates of the atoms and the secondary structure of the peptide chains for beginning of the simulation can be taken from a resource such as Protein Data Bank (PDB) or obtained from an all-atom simulation of the peptide chains. Here we used the second way. We used the final configuration of the two peptide chains in an all-atom simulation of the double-chain system of EAK16-I for producing the system's initial configuration for the coarse-grained simulation. Regarding the behavior of the system on the double-chain level, we generated several copies of the coarse-grained version of the two chains to prepare the initial configuration of the system's many-chain simulation. Then we filled the rest of the simulation box with coarse-grained water molecules of the MARTINI model and started the simulation. In the case of EAK16-IV, taking the results of the all-atom simulation of the single-chain system into consideration, copies of the coarse-grained version of single peptides were used for preparing the system initial configuration in the many-chain simulations on the coarse-grained level. Coarse-grained simulations were performed in the NPT ensemble with periodic boundary conditions in three dimensions. The peptides and water were coupled separately to a heat bath at 300°K ($\tau_T = 0.3$ ps), and the system was isotropically coupled to a pressure bath at 1 bar ($\tau_P = 3$ ps) with the Berendsen method (Berendsen et al. 1984). Electrostatic interactions were calculated using the Shift method. Prior to the main simulations, the systems were energy minimized (5000-step steepest descent), followed by 1 ns simulation in the NVT ensemble.

Results and discussion

Experimental observations

An AFM is used to observe the assemblies of EAK16-II and EAK16-IV peptides. AFM images of the assemblies are shown in Fig. 1. As can be seen in these images of 2×2-μm^2 scan size, EAK16-II and EAK16-IV peptides form fibrillar and globular assemblies, respectively. Some globular structures can also be seen in the case of EAK16-II together with the fibers. These results are in agreement with the experimental observations reported in Jun et al. (2004). Measurements over AFM images show that the fibrillar assemblies of EAK16-II peptide are typically 8 nm wide, 2.5 nm high and 100–200 nm long.

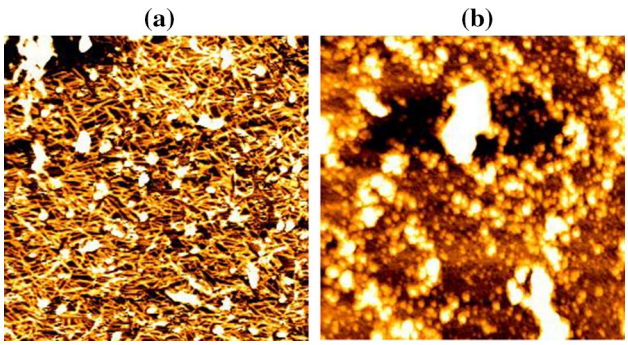

Fig. 1 AFM images of the assemblies of EAK16-II (**a**) and EAK16-IV (**b**) at neutral pH and a concentration of 0.1 mg/ml. As can be seen, EAK16-II is assembled into fibrillar structures, and EAK16-IV forms globular assemblies. The scan size of the images is 2×2 μm^2

It has been shown experimentally that the self-assembly behavior of EAK16-I is very similar to that of EAK16-II (Jun et al. 2004). At neutral pH, EAK16-I peptides assemble into fibrillar structures very similar to the representation in Fig. 1a. It seems that understanding the mechanism of fiber formation in the solution of EAK16-I or EAK16-II would give insight about the other ones. Accordingly, our results obtained from simulations of EAK16-I peptide can be generalized to EAK16-II peptide.

Single-chain all-atom simulations

For each single EAK16-I and EAK16-IV peptide chain, we carry out three simulations of 250-ns time length with different initial velocities of atoms for checking the repeatability of the results. Parameters such as root mean square deviation (RMSD), radius of gyration, R_g and end-to-end distance, R_e, of the peptide chains are measured in the course of the simulations. Also, time-averaged separations between amino acids of each peptide chain are calculated. In Fig. 2, RMSD, R_g and R_e for the three simulations of the two peptides EAK16-I and EAK16-IV are shown. As can be seen in this figure, EAK16-IV peptide reaches a persistent configuration after about 100 ns. After that, the configuration of this peptide has small fluctuations. In the case of EAK16-I peptide, however, there is no significant persistent configuration, and structural fluctuations are quite considerable along the simulation. EAK16-I has a larger radius of gyration and end-to-end distance in most of the simulation times relative to EAK16-IV, showing that EAK16-I has a larger spatial expansion compared with EAK16-IV.

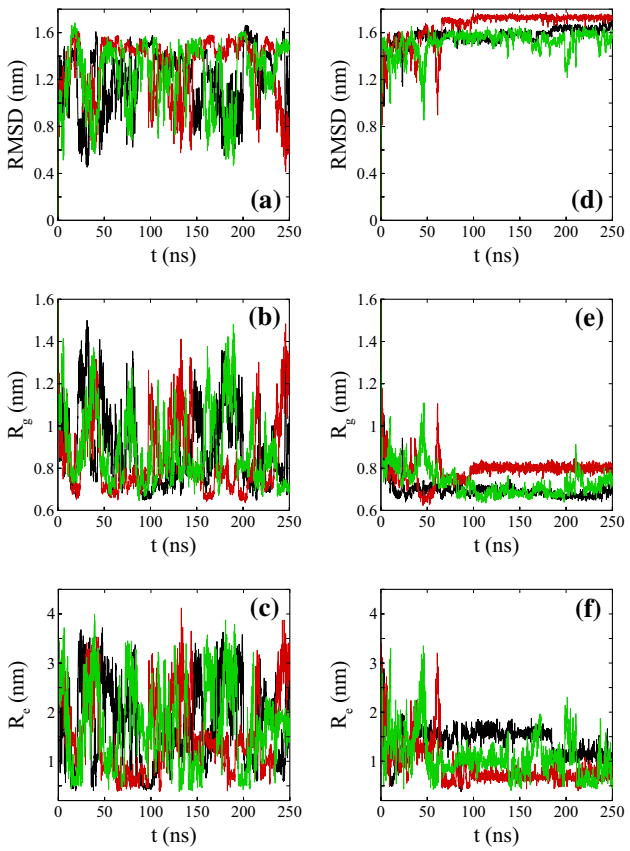

Fig. 2 RMSD, radius of gyration and end-to-end distance of EAK16-I (**a–c**) and EAK16-IV (**d–f**), respectively. *Black, red* and *green colors* show the results obtained from three runs of the simulations of each peptide chain with three different initial velocities of their atoms for checking repeatability of the results

In fact, strong intra-chain electrostatic interactions in EAK16-IV peptide cause it to take a folded conformation, and the thermal fluctuations are not capable of changing it noticeably. In the case of EAK16-I peptide, however, lack of such strong intra-chain electrostatic interactions causes the thermal fluctuations to change the peptide conformation easily.

In order to obtain more information about the peptide conformations, the density plots of the time-averaged separation between the amino acids of the peptide chains are shown in Fig. 3. The separations between amino acids are averaged over time from $t = 150$ ns to $t = 250$ ns. It has been checked that averaging over other time intervals (for example, from $t = 200$ ns to $t = 250$ ns) gives similar results. In each panel of this figure, the grayscale of the square in row i and column j reflects the time-averaged separation between amino acids i and j of the peptide chain. The darker the square in row i and column j, the larger the time-averaged separation between amino acids i and j the corresponding peptide chain. It should be noted that a large and positive gradient of the darkness of squares in the first row of each panel shows that the corresponding chain has dominantly extended conformation (see Fig. 3a, for example). A light region perpendicular to the main diagonal of a panel shows that the corresponding chain has a dominantly curved (or hairpin-shaped) conformation (see Fig. 3e, for example). It can be concluded from the panels of Fig. 3 that the EAK16-I chain experiences dominantly extended conformation for most of the simulation time. The EAK16-IV chain, however, takes a folded hairpin-shaped conformation along most of the simulation time. Snapshots of the final conformation of each peptide in the simulations are shown in Fig. 4.

Double chain all-atom simulations

As mentioned above, the EAK16-I chain has a dominantly extended conformation in the solution in neutral pH conditions. Emamyari and Fazli (2014b) showed that when two chains of EAK16-I (or EAK16-II) reach each other in a solution of neutral pH and form a dimer, the extended conformation of the chains does not change, and the dimer continues to have an extended

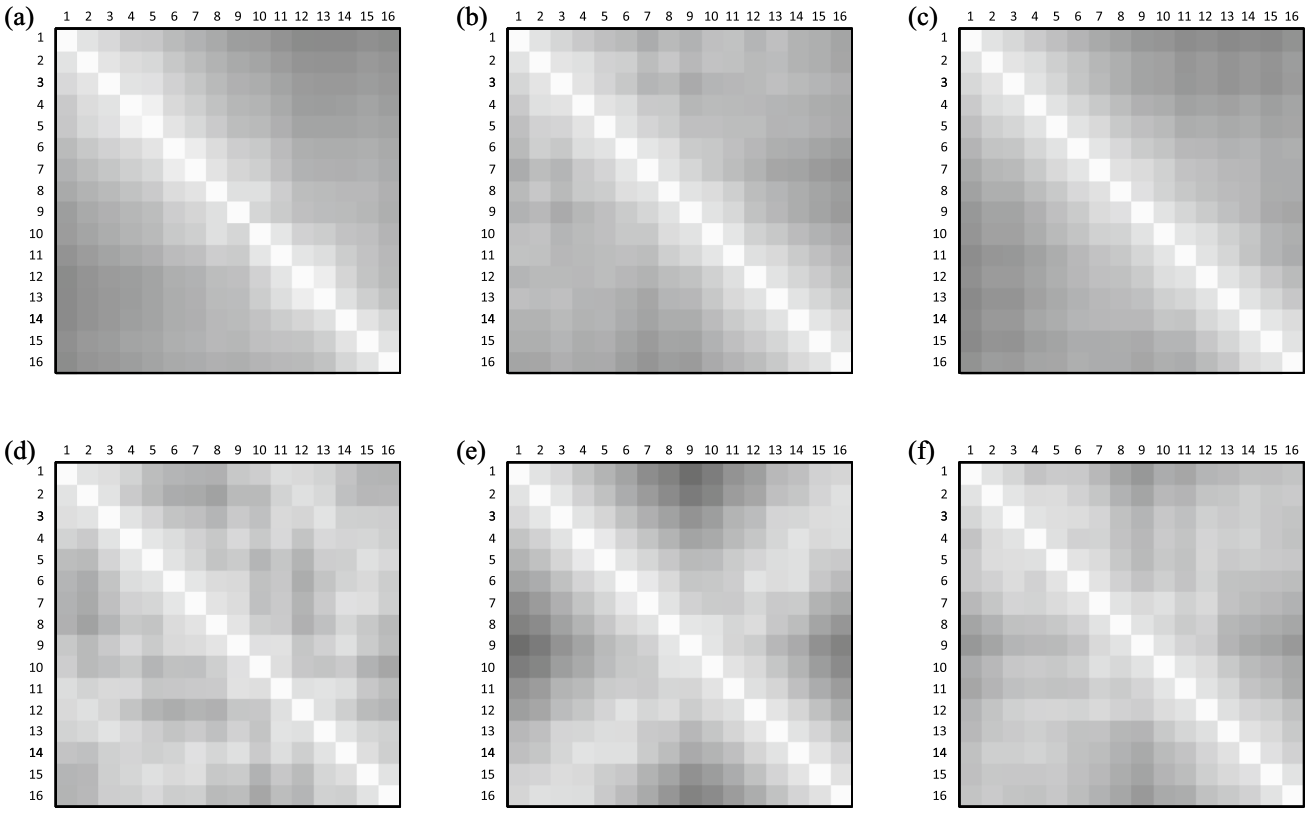

Fig. 3 Density plots of the time-averaged separations between pairs of amino acids of peptide chains for EAK16-I (**a–c**) and EAK16-IV (**d–f**). The averages are calculated over time from $t = 150$ ns to $t = 250$ ns. *Darkness of the squares*, which corresponds to the separation between amino acids, ranges from 0 to 2.32 nm

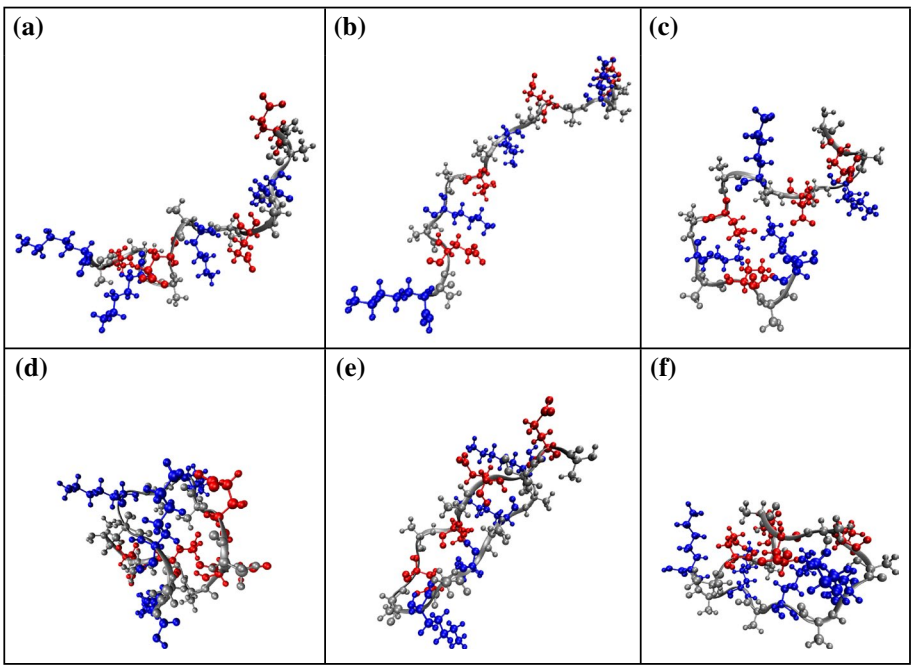

Fig. 4 The final snapshots of single EAK16-I (**a–c**) and EAK16-IV (**d–f**) chains obtained from three repetitions of all-atom simulations. The backbones of the chains and alanines are shown in *gray*, and lysines and glutamic acids are shown in *blue* and *red*, respectively. Water molecules are not shown for clarity

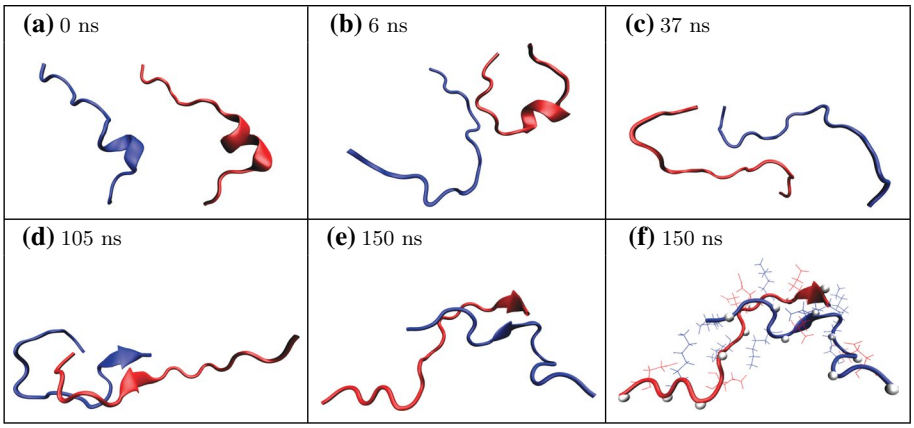

Fig. 5 Sequential snapshots of the two EAK16-I peptide chains in an all-atom simulation of the double-chain system. Only the backbones of the chains with assigned secondary structures are shown for clarity (**a**–**e**). The final conformation of the chains including their backbone and the side chains in which lysines, glutamic acids and alanines are shown in *blue*, *red* and *white*, respectively (**f**)

conformation. Although single-chain simulations show that the EAK16-I chain has an extended conformation for most of the simulation time, for double-chain simulations we prepare an extreme initial configuration in which the two EAK16-I chains are close to each other as they have a non-extended conformation. We choose two configurations from two moments of single-chain simulations in which the EAK16-I chain has an α-helix part, and we start a double-chain simulation from the initial configuration shown in Fig. 5a. An all-atom simulation of the system containing the two chains shows that the α-helix parts of the chains disappear gradually as time lapses, and an antiparallel β-sheet is formed by the two chains, as shown in Fig. 5. In fact, the α-helix to β-sheet transition happens in the course of the dimerization of EAK16-I peptide. We use the final conformation of the two chains in an all-atom simulation of the double-chain system to construct their coarse-grained version for use in the simulation of the many-chain system. One should note here that the lower propensity of the chains to an α-helix relative to a β-sheet is a signature of their tendency fo fibril formation (Chiti and Dobson 2006).

As a signature of the hydrophobic interaction between the two peptide chains, we calculate the radial distribution function (rdf) of the hydrophobic monomers (alanines) of one chain relative to that of the other. As shown in Fig. 6, alanine amino acids of the two chains are mostly close to each other, and the most probable separation between them is 0.5 nm. Accordingly, the two chains have a hydrophobic tendency toward each other, and the interplay between this tendency and the entropic effects results in the formation of a β-sheet region along the chains as they have an extended conformation (see Fig. 5f).

In the case of EAK16-IV, as mentioned above, the strong intra-chain electrostatic interactions fold a single chain into a hairpin-shaped conformation in the neutral pH condition. It is expected that two chains of this type reach each other in the solution dominantly as two hairpin-shaped

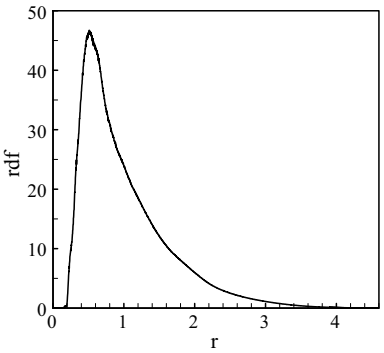

Fig. 6 Radial distribution function (rdf) of alanines of one EAK16-I chain relative to alanines of the other chain in a double-chain simulation of EAK16-I

chains; the main interaction between them is hydrophobic (because their hydrophobic side chains are shown in single-chain simulations that are exposed to water, as has also been reported in Ref. Emamyari and Fazli 2014b). To show that the tendency of EAK16-IV chains to interact with each other in this manner is strong, we start an all-atom simulation of the double-chain system of this peptide from an initial configuration in which the two chains are not completely folded and have a curved conformation instead. To this end, we choose two non-folded single-chain conformations from single-chain simulations and copy them to the box of the double-chain simulation, as shown in Fig. 7a. Then we start an all-atom simulation of the double-chain system and probe the conformational evolution of the peptide chains. Our results show that as time lapses, the two chains do not show a tendency to attract each other in an extended conformation. Instead, they take folded conformations individually, and the main interaction between them is a weak hydrophobic interaction. As shown in Fig. 7f, at the end of this simulation, one of the chains has a hairpin-shaped conformation and the other has a curved conformation with a part in α-helix form. This behavior is

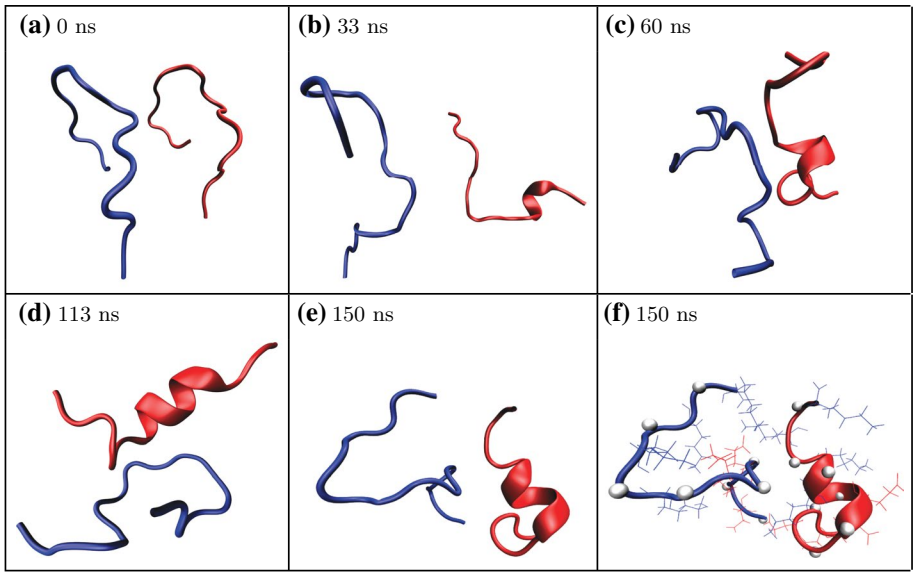

Fig. 7 Sequential snapshots of the two EAK16-IV peptide chains in an all-atom simulation of the double-chain system. Only the backbones of the chains with assigned secondary structures are shown for clarity (**a**–**e**). The final conformation of the chains, including the backbone of the chains and the side chains with lysines, glutamic acids and alanines, are shown in *blue*, *red* and *white*, respectively (**f**)

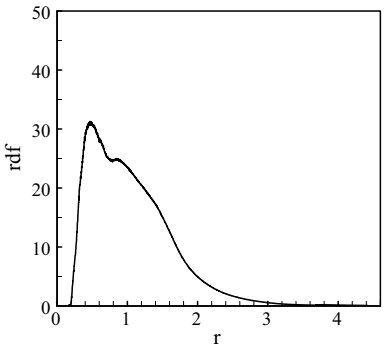

Fig. 8 Radial distribution function (rdf) of alanines of one EAK16-IV chain relative to alanines of the other chain in a double-chain simulation of EAK16-IV

quite different from the behavior of EAK16-I on the double-chain level.

The radial distribution function of the alanines of the two chains relative to each other is calculated and is shown in Fig. 8. As can be concluded from this figure, the probability of the presence of alanines of a chain close to alanines of the other chain is smaller than that in the case of EAK16-I chains. This result shows that unlike the case of EAK16-I, there is no region of considerable length between the two chains with a hydrophobic interaction between them. Because of the folded conformation of the two EAK16-IV chains, only a small region of them can have hydrophobic interaction.

Coarse-grained simulation of many-chain systems

As mentioned above, two EAK16-I chains find each other in the solution and form an antiparallel β-sheet in the contact region. Thus, we take the coordinates of the atoms and the secondary structure of the two EAK16-I peptides from the final stage of double-chain all-atom simulations and construct their coarse-grained version. Then we generate a number of copies of the coarse-grained dimers in the simulation box to prepare the initial conformation of the system for coarse-grained simulation of a many-chain system. The secondary structure of the two chains (A and B), which are determined using the DSSP program (Kabsch and Sander 1983), are as follows.

Chain A: CCCCCCCEEEEEECC
Chain B: CCCCCCCCCEEEEECC

Here, C and E mean the coil and extended-beta, respectively. A solvent with 8 dimers (16 peptides) and 31,808 water molecules in a cubic box of edge length 10 nm is prepared for the simulation. This system is simulated for 200 ns for extracting the results. The time evolution of the total energy of the system is shown in Fig. 9a. The total energy decreases as the time lapses and after about 70 ns fluctuates around an approximately constant value. This shows that the system reaches to a stable state with minimum energy. Figure 9b also shows the time evolution of the number of clusters in the system. Two EAK16-I chains are considered to belong to a cluster if they have a distance smaller than 0.5 nm from each other. As can be seen, the number of clusters at the beginning of the simulation is 8 (8 pairs of EAK16-I peptide chains), and after about 70 ns it reaches to 1 and remains fixed until the end of the simulation. Thus, all of the peptides aggregate and form a single cluster in the system.

The signature of the assembling process can also be seen from the density profile of the peptide chains, which is drawn along three Cartesian axes, x, y and z (see Fig. 10).

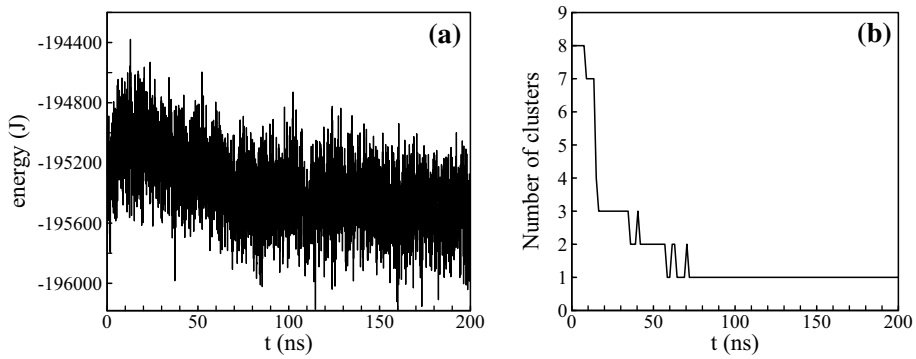

Fig. 9 Time evolution of the total energy of the system (**a**) and the number of clusters in the system (**b**) in a coarse-grained simulation of eight pairs of EAK16-I chains. As can be seen, as time passes, coarsening of the clusters happens, and finally all the chains form a single cluster. The aggregation process decreases the total energy of the system as is expected

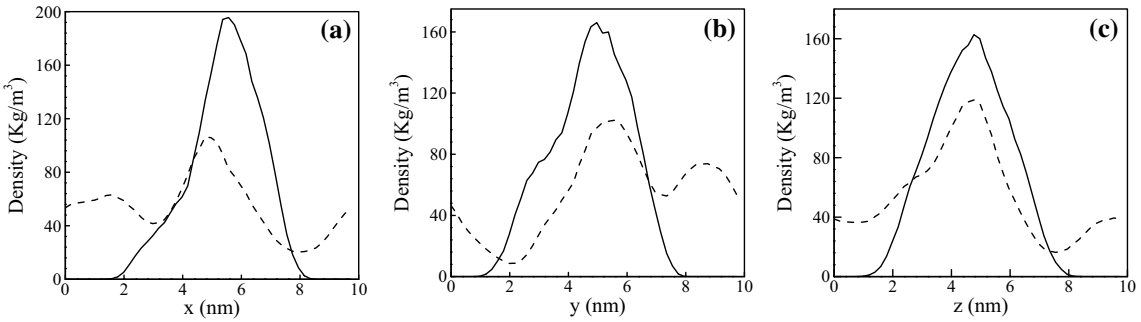

Fig. 10 Density maps of the particles in the system of eight pairs of EAK16-I chains in x (**a**), y (**b**) and z (**c**) directions before (*dashed line*) and after (*solid line*) assembly of the peptides into a single cluster. *Dashed* and *solid lines* are obtained from averaging the density over the first and the last 30 ns of the simulation time, respectively

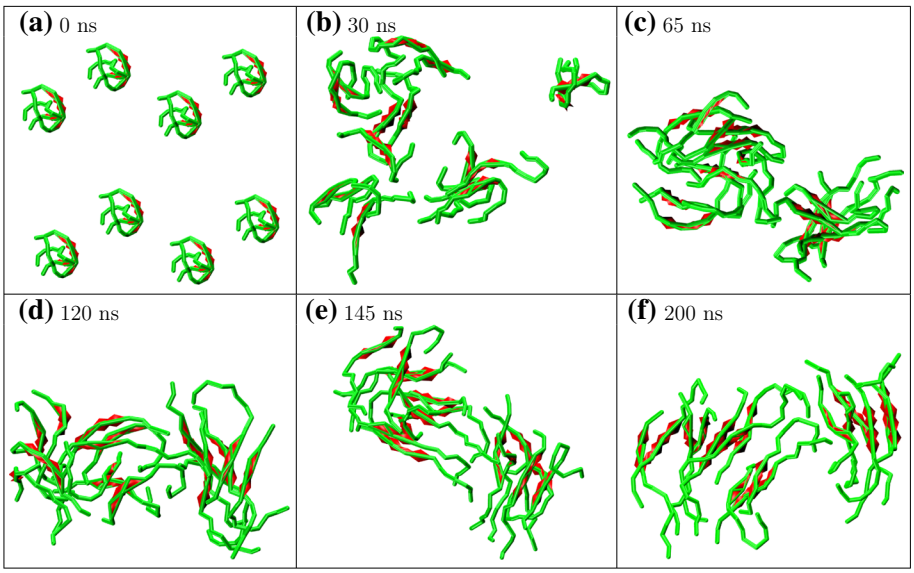

Fig. 11 Sequential snapshots from a coarse-grained simulation of eight pairs of EAK16-I peptide (**a**–**f**). β-Sheets formed by the pairs of the peptide chains are shown in *red*. The tendency of β-sheets to stack over each other and form fiber-like assemblies can be clearly seen in the system

Before the aggregation process, the density profiles are broad, but at the end of the simulation they are sharper, meaning that the peptides are placed in a small region in the simulation box as a single cluster.

Some snapshots of the system in this simulation are shown in Fig. 11 from the beginning to the end of the simulation. As can be seen, peptides aggregate and finally form a single assembly. β-Sheets are shown in red in this figure. It can be seen that β-sheets of the dimers are mostly close and parallel to each other in the final assembly. In fact, even with such a small number of peptide dimers, the tendency of the β-sheets of the dimers to stack over each

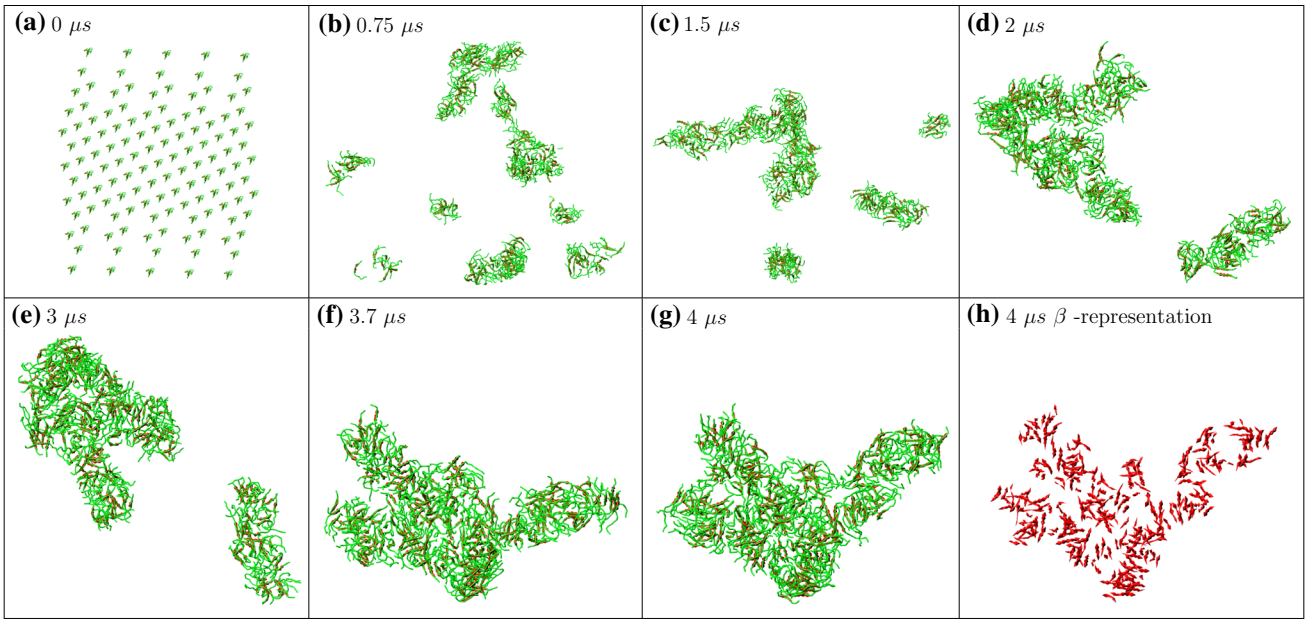

Fig. 12 Sequential snapshots of the system in a coarse-grained simulation of 250 (125 pairs) EAK16-I peptides. β-Sheets formed by the peptide pairs are shown in *red*. Tendency of β-sheets to stack over each other and form fiber-like assemblies can be clearly seen in the system

other and form a fiber-like assembly can be clearly seen. To further check the mentioned tendency in the dimer system, we simulate a larger system containing 125 dimers of the peptides (250 peptides) in a cubic simulation box of 32-nm dimensions, which contains 281,750 coarse-grained water molecules. The time step in this simulation is 20 fs, and the total simulation time is 4 μs. Sequential snapshots from this simulation are shown in Fig. 12. In this figure, indications of fibrillar growth of the nucleated assemblies can be seen in panels (b–g). In Fig. 12e a "U" -shaped fibrillar assembly and a shorter fiber-shaped assembly can be seen, which finally come close to each other, as can be seen in Fig. 12g. β-Sheets of the peptide pairs of panel (g) are shown in panel (h). From the results of coarse-grained simulations, rough estimates can be made about the dimensions of the formed fibrillar assemblies. The results show that the thickness of the fibrillar assemblies is about one to two peptide lengths (5–10 nm), in reasonable agreement with the experiment.

The mechanism of fiber formation and the role of β-sheets in this process have been studied by numerous research groups. For example, it has been shown using high-resolution solid-state NMR that fibrillation happens through lateral elongation of β-sheet bilayers (Cormier et al. 2013). Also, existing β-sheets causing the conformational transition of other non-beta peptides has also been shown (Wen et al. 2014b).

However, EAK16-I and two EAK16-IV chains do not show a strong tendency to attract each other and form a stable dimer with specified structure. Therefore, in the coarse-graining stage of EAK16-IV peptide, we take the coordinates of atoms of only a single chain and assign the secondary structure to it. Then we generate copies of the coarse-grained version of this chain in the simulation box. The secondary structure assigned to the EAK16-IV chain at the end of an all-atom simulations is:

CCEEECCSSSCCEEEC

in which C, E and S mean coil, extended-beta and bend, respectively. A solution containing 125 coarse-grained EAK16-IV peptides and 1,25,250 water molecules in a cubic box of 24.5-nm dimensions is prepared for simulation. The time step in this simulation is 20 fs, and the total simulation time is 2.1 μs. Sequential snapshots from the simulation are shown in Fig. 13. As can be seen, the coarse-grained EAK16-IV chains aggregate into a single cluster as the time lapses. As can be seen from two views of the final aggregate, an assembly with no special shape is formed in which no order of the chains and the small sections of extended-beta can be observed. The final aggregate is approximately a disk-shaped assembly.

One should note here that considering the dimers as the units of peptides in the simulation of the many-chain system of EAK16-I is based on our observation in all-atom simulations of the double-chain system of this peptide. In light of the facts that in the beginning of the self-assembly the most probable interaction is that between the single chains and that couples of the peptides form very stable dimers, considering the many-chain system as composed of the dimers looks feasible. Clearly, joining of single peptides or assemblies containing odd numbers of the peptides

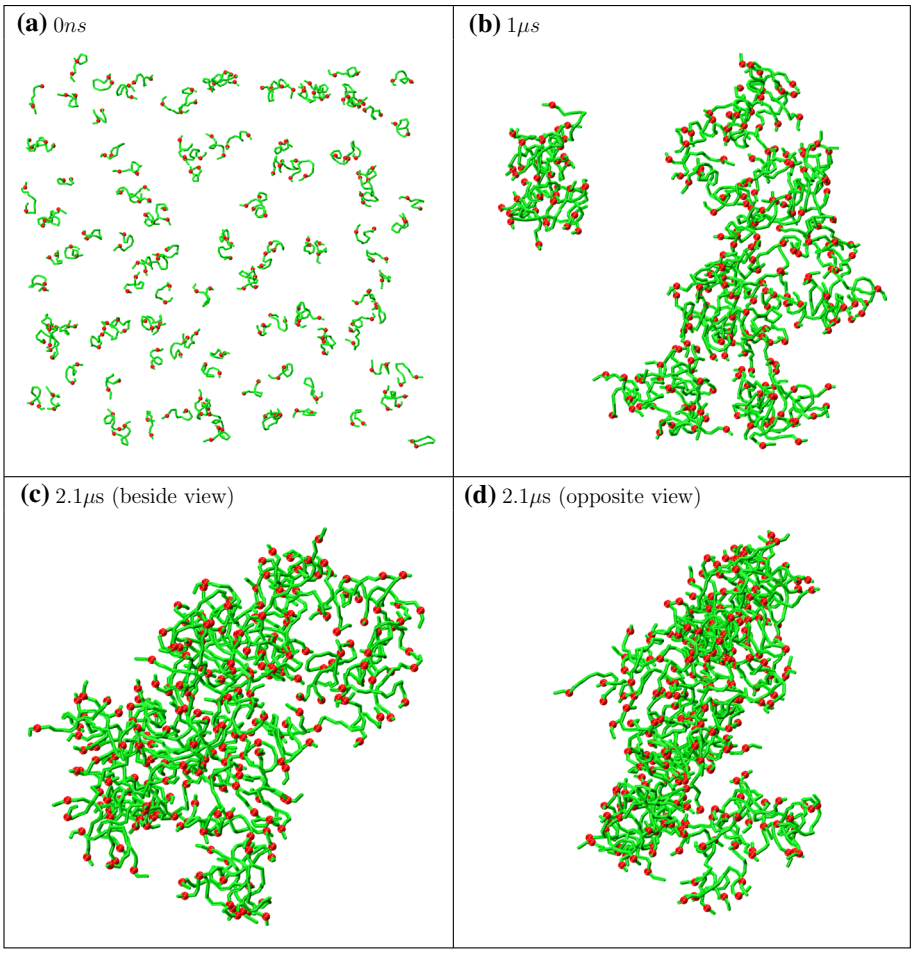

Fig. 13 Snapshot from the system in a coarse-grained simulation of 125 EAK16-IV chains. Short sections of β-strands of the chains are shown in *red*

to the assemblies containing even numbers of the peptides happens in reality. We eliminated such a possibility in our simulation based on our observations.

Conclusions

In conclusion, the phenomenon of the self-assembly of EAK16-family peptides has been studied using a combination of all-atom and coarse-grained molecular dynamics simulations to cover a temporal range from nano- to micro-seconds. Following Jun et al. (2004), a self-assembly experiment of EAK16-II and EAK16-IV peptides in neutral pH conditions was been performed, and formation of fibrillar assemblies by EAK16-II and globular assemblies by EAK16-IV was observed. It has been shown that the approach of using all-atom simulations on the single- and double-chain levels and coarse-grained simulations on the many-chain level predicts the experimental observations reasonably well. Simulations of EAK16-I peptide showed that the tendency of this peptide on the double-chain level for formation of β-sheets provides the possibility of formation of fibrillar assemblies on the many-chain level. Staking of β-sheets formed by pairs of peptides over each other and signatures of the formation of fibrils in coarse-grained simulations of EAK16-I were observed. In the case of EAK16-IV, however, the tendency of single chains to have a hairpin-shaped folded conformation, which arises from strong intra-chain electrostatic interactions, was shown to cause the formation of globular assemblies on the many-chain level. The self-assembly process of EAK16-I and EAK16-IV peptides from the single- to many-chain levels are shown schematically in Fig. 14.

As stated before, one of the main conclusions that can be drawn from studies on model peptides such as EAK16 is the extent to which the results can help to explain what happens in molecular terms concerning the aggregative behavior of peptides, such as beta amyloid peptide (Aβ), whose aggregation and fibrillation, according to the amyloid cascade hypothesis, are the main reason for devastating diseases such as Alzheimer's disease. Comparing the amino acid sequences of EAK16 peptides studied here with the amino acid sequence of Aβ shows that there is a strong homology between EAK16-II and the N-terminal region of Aβ in terms of charge distribution (Fig. 15, blue and red colors, positively and negatively charged amino

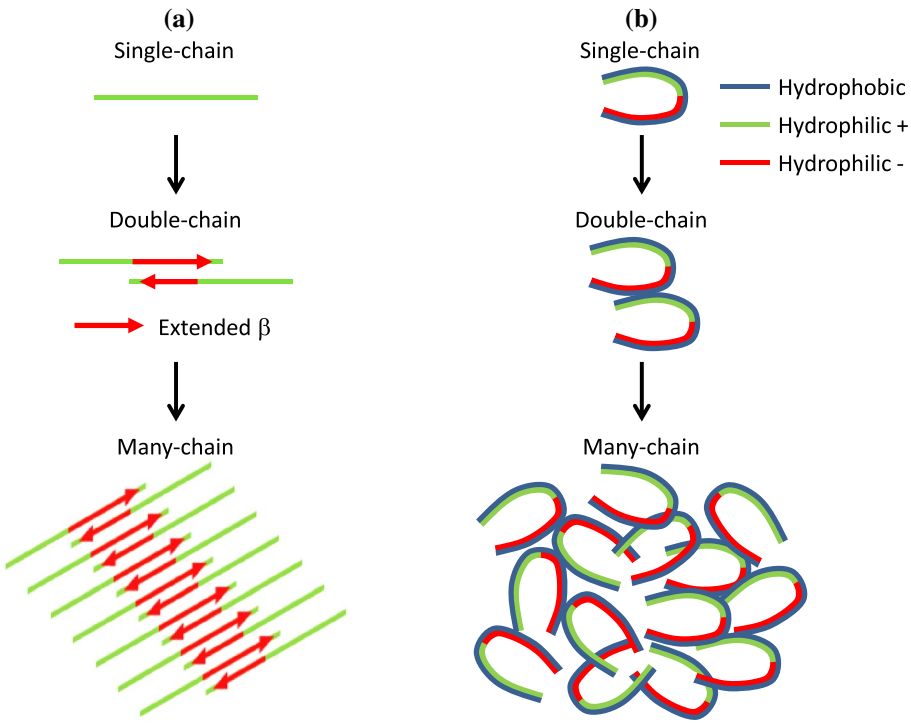

Fig. 14 Schematic representation of the self-assembly process of EAK16-I (**a**) and EAK16-IV (**b**) from single- to many-chain levels

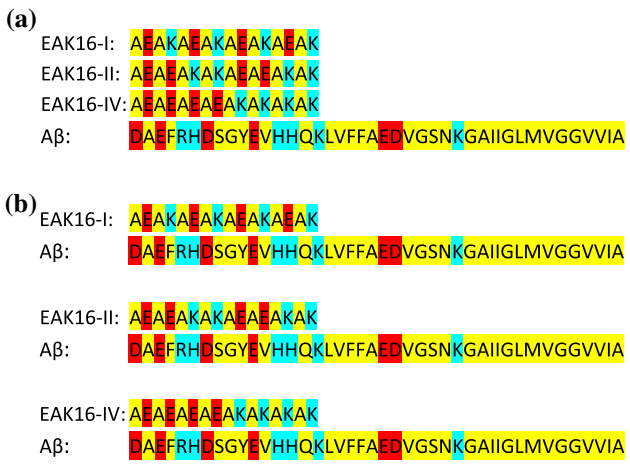

Fig. 15 The amino acid sequence of EAK16 peptides and Aβ (**a**) and a comparison between them (**b**). Hydrophobic, negatively charged and positively charged residues are shown by *yellow*, *red* and *blue colors*, respectively. As can be seen, there is a strong homology between charge distributions of EAK16-II and the N-terminal region of Aβ

acids, respectively). Also, half of the residues in EAK16-II peptide and almost half of the residues in the N-terminal end of Aβ are hydrophobic (Fig. 15, yellow colors). In EAK16-II there is an alternative sequence of two negative and two positive charges, interspersed with hydrophobic residues. Almost the same order can be seen in the N-terminal half of Aβ, with differences mainly in the interspersed hydrophobic residues. Also, since the clustering of hydrophobic residues promotes the aggregation of proteins and peptides (Chiti and Dobson 2006), and these two peptides are also comparable in this regard, we can state and emphasize the possible importance of this arrangement of amino acids at least in the initial steps of the aggregation and fibrillation of amyloid peptides. Of course, the whole process of derivation of relatively high concentrations of highly toxic amyloid oligomers and also the generation of amyloid fibrils in the brain of AD patients are much more complex phenomena; understanding them would be much easier if the initial steps were clarified. Here we propose that, according to our findings and the above comparison, the charge distribution and hydrophobic arrangement, homologous to EAK16-II, could be operative and determinative in the initial steps of the generation of pathologic Aβ oligomers and fibrils.

References

Aggeli A, Nyrkova IA, Bell M, Harding R, Carrick L, McLeish TCB, Semenov AN, Boden N (2001) Hierarchical self-assembly of chiral rod-like molecules as a model for peptide beta-sheet tapes, ribbons, fibrils, and fibers. Proc Natl Acad Sci USA 98:11857–11862. doi:10.1073/pnas.191250198

Benilova I, Karran E, De Strooper B (2012) The toxic Aβ oligomer and Alzheimer's disease: an emperor in need of clothes. Nat Neurosci 15:349–357. doi:10.1038/nn.3028

Berendsen HJC, Postma JPM, van Gunsteren WF, Hermans J (1981) Interaction models for water in relation to protein

hydration. Intermolecular forces. D. Reidel Publishing Company, Dordrecht, p 331–342. doi: 10.1007/978-94-015-7658-1_21
Berendsen HJC, Postma JPM, van Gunsteren WF, DiNola A, Haak JR (1984) Molecular dynamics with coupling to an external bath. J. Chem. Phys. 81:3684–3690. doi:10.1063/1.448118
Bowerman CJ, Nilsson BL (2012) Review self-assembly of amphipathic β-sheet peptides: insights and applications. Biopolymers 98:169–184. doi:10.1002/bip.22058
Chen J, Pompano RR, Santiago FW, Maillat L, Sciammas R, Sun T, Han H, Topham DJ, Chong AS, Collier JH (2013) The use of self-adjuvanting nanofiber vaccines to elicit high-affinity B cell responses to peptide antigens without inflammation. Biomaterials 34:8776–8785. doi:10.1016/j.biomaterials.2013.07.063
Chiti F, Dobson CM (2006) Protein misfolding, functional amyloid, and human disease. Annu Rev Biochem 75:333–366. doi:10.1146/annurev.biochem.75.101304.123901
Claussen RC, Rabatic BM, Stupp SI (2003) Aqueous self-assembly of unsymmetric peptide bolaamphiphiles into nanofibers with hydrophilic cores and surfaces. J Am Chem Soc 125:12680–12681. doi:10.1021/ja035882r
Colombo G, Soto P, Gazit E (2007) Peptide self-assembly at the nanoscale: a challenging target for computational and experimental biotechnology. Trends Biotechnol 25:211–218. doi:10.1016/j.tibtech.2007.03.004
Cormier AR, Pang X, Zimmerman MI, Zhou H-X, Paravastu AK (2013) Molecular structure of RADA16-I designer self-assembling peptide nanofibers. ACS Nano 7:7562–7572. doi:10.1021/nn401562f
Darden T, York D, Pedersen L (1993) Particle mesh Ewald: an N log (N) method for Ewald sums in large systems. J Chem Phys 98:10089–10092. doi:10.1063/1.464397
Emamyari S, Fazli H (2014a) pH-dependent self-assembly of EAK16 peptides in the presence of a hydrophobic surface: coarse-grained molecular dynamics simulation. Soft Matter 10:4248–4257. doi:10.1039/c4sm00307a
Emamyari S, Fazli H (2014b) All-atom molecular dynamics study of EAK16 peptide: the effect of pH on single-chain conformation, dimerization and self-assembly behavior. Eur Biophys J 43:143–155. doi:10.1007/s00249-014-0949-x
Essmann U, Perera L, Berkowitz ML, Darden T, Lee H, Pedersen LG (1995) A smooth particle mesh Ewald method. J Chem Phys 103:8577–8593. doi:10.1063/1.470117
Galler KM, Cavender A, Yuwono V, Dong H, Shi S, Schmalz G, Hartgerink JD, D'Souza RN (2008) Self-assembling peptide amphiphile nanofibers as a scaffold for dental stem cells. Tissue Eng Part A 14:2051–2058. doi:10.1089/ten.tea.2007.0413
Haass C, Selkoe DJ (2007) Soluble protein oligomers in neurodegeneration: lessons from the Alzheimer's amyloid beta-peptide. Nat Rev Mol Cell Biol 8:101–112. doi:10.1038/nrm2101
Harper JD, Lieber CM, Lansbury PT (1997a) Atomic force microscopic imaging of seeded fibril formation and fibril branching by the Alzheimer's disease amyloid-β protein. Chem Biol 4:951–959. doi:10.1016/S1074-5521(97)90303-3
Harper JD, Wong SS, Lieber CM, Lansbury PT (1997b) Observation of metastable Aβ amyloid protofibrils by atomic force microscopy. Chem Biol 4:119–125. doi:10.1016/S1074-5521(97)90255-6
Hartgerink JD, Beniash E, Stupp SI (2002) Peptide-amphiphile nanofibers: a versatile scaffold for the preparation of self-assembling materials. Proc Natl Acad Sci USA 99:5133–5138. doi:10.1073/pnas.072699999
Hess B, Bekker H, Berendsen HJC, Fraaije JGEM (1997) LINCS: a linear constraint solver for molecular simulations. J Comput Chem 18:1463–1472. doi:10.1002/(SICI)1096-987X(199709)18:12<1463:AID-JCC4>3.0.CO;2-H
Hess B, Kutzner C, van der Spoel D, Lindahl E (2008) GROMACS 4: algorithms for highly efficient, load-balanced, and scalable molecular simulation. J Chem Theory Comput 4:435–447. doi:10.1021/ct700301q
Holmes TC (2002) Novel peptide-based biomaterial scaffolds for tissue engineering. Trends Biotechnol 20:16–21. doi:10.1016/S0167-7799(01)01840-6
Hong Y, Legge RL, Zhang S, Chen P (2003) Effect of amino acid sequence and pH on nanofiber formation of self-assembling peptides EAK16-II and EAK16-IV. Biomacromolecules 4:1433–1442. doi:10.1021/bm0341374
Hong Y, Lau LS, Legge RL, Chen P (2004) Critical self-assembly concentration of an ionic-complementary peptide EAK16-I. J Adhes 80:913–931. doi:10.1080/00218460490508616
Hong Y, Pritzker MD, Legge RL, Chen P (2005) Effect of NaCl and peptide concentration on the self-assembly of an ionic-complementary peptide EAK16-II. Colloids Surf B Biointerfaces 46:152–161. doi:10.1016/j.colsurfb.2005.11.004
Humphrey W, Dalke A, Schulten K (1996) VMD: visual molecular dynamics. J Mol Graph 14:33–38. doi:10.1016/0263-7855(96)00018-5
HyperChem (TM) Hypercube Inc., 1115 NW 4th Street, Gainesville, Florida 32601, USA
Izvekov S, Voth GA (2005) A multiscale coarse-graining method for biomolecular systems. J Phys Chem B 109:2469–2473. doi:10.1021/jp044629q
Jorgensen WL, Tirado-Rives J (1988) The OPLS potential functions for proteins. Energy minimizations for crystals of cyclic peptides and crambin. J Am Chem Soc 110:1657–1666. doi:10.1021/ja00214a001
Jun S, Hong Y, Imamura H, Ha B-Y, Bechhoefer J, Chen P (2004) Self-assembly of the ionic peptide EAK16: the effect of charge distributions on self-assembly. Biophys J 87:1249–1259. doi:10.1529/biophysj.103.038166
Kabsch W, Sander C (1983) Dictionary of protein secondary structure: pattern recognition of hydrogen-bonded and geometrical features. Biopolymers 22:2577–2637. doi:10.1002/bip.360221211
Kayed R, Sokolov Y, Edmonds B, McIntire TM, Milton SC, Hall JE, Glabe CG (2004) Permeabilization of lipid bilayers is a common conformation-dependent activity of soluble amyloid oligomers in protein misfolding diseases. J Biol Chem 279:46363–46366. doi:10.1074/jbc.C400260200
Kokkoli E, Mardilovich A, Wedekind A, Rexeisen EL, Garg A, Craig JA (2006) Self-assembly and applications of biomimetic and bioactive peptide-amphiphiles. Soft Matter 2:1015–1024. doi:10.1039/B608929A
Koutsopoulos S, Zhang S (2012) Two-layered injectable self-assembling peptide scaffold hydrogels for long-term sustained release of human antibodies. J Controll Release 160:451–458. doi:10.1016/j.jconrel.2012.03.014
Koutsopoulos S, Unsworth LD, Nagai Y, Zhang S (2009) Controlled release of functional proteins through designer self-assembling peptide nanofiber hydrogel scaffold. Proc Natl Acad Sci USA 106:4623–4628. doi:10.1073/pnas.0807506106
Levine RM, Scott CM, Kokkoli E (2013) Peptide functionalized nanoparticles for nonviral gene delivery. Soft Matter 9:985–1004. doi:10.1039/C2SM26633D
Marrink SJ, Risselada HJ, Yefimov S, Tieleman DP, de Vries AH (2007) The MARTINI force field: coarse grained model for biomolecular simulations. J Phys Chem B 111:7812–7824. doi:10.1021/jp071097f
Miyamoto S, Kollman PA (1992) SETTLE: an analytical version of the SHAKE and RATTLE algorithms for rigid water models. J Comput Chem 13:952–962. doi:10.1002/jcc.540130805
Monticelli L, Kandasamy SK, Periole X, Larson RG, Tieleman DP, Marrink SJ (2008) The MARTINI coarse-grained force field: extension to proteins. J Chem Theory Comput 4:819–834. doi:10.1021/ct700324x

Naiki H, Hashimoto N, Suzuki S, Kimura H, Nakakuki K, Gejyo F (1997) Establishment of a kinetic model of dialysis-related amyloid fibril extension in vitro. Amyloid 4:223–232. doi:10.3109/13506129709003833

Pedersen JS, Christensen G, Otzen DE (2004) Modulation of S6 fibrillation by unfolding rates and gatekeeper residues. J Mol Biol 341:575–588. doi:10.1016/j.jmb.2004.06.020

Peter C, Kremer K (2009) Multiscale simulation of soft matter systems from the atomistic to the coarse-grained level and back. Soft Matter 5:4357–4366. doi:10.1039/B912027K

Roychaudhuri R, Yang M, Hoshi MM, Teplow DB (2009) Amyloid β-protein assembly and Alzheimer disease. J Biol Chem 284:4749–4753. doi:10.1074/jbc.R800036200

Rudra JS, Tian YF, Jung JP, Collier JH (2010) A self-assembling peptide acting as an immune adjuvant. Proc Natl Acad Sci USA 107:622–627. doi:10.1073/pnas.0912124107

Serio TR, Cashikar AG, Kowal AS, Sawicki GJ, Moslehi JJ, Serpell L, Arnsdorf MF, Lindquist SL (2000) Nucleated conformational conversion and the replication of conformational information by a prion determinant. Science 289:1317–1321. doi:10.1126/science.289.5483.1317

Sheng Y, Wang W, Chen P (2010a) Adsorption of an ionic complementary peptide on the hydrophobic graphite surface. J Phys Chem C 114:454–459. doi:10.1021/jp908629g

Sheng Y, Wang W, Chen P (2010b) Interaction of an ionic complementary peptide with a hydrophobic graphite surface. Protein Sci 19:1639–1648. doi:10.1002/pro.444

Shi Q, Izvekov S, Voth GA (2006) Mixed atomistic and coarse-grained molecular dynamics: simulation of a membrane-bound ion channel. J Phys Chem B 110:15045–15048. doi:10.1021/jp062700h

Thøgersen L, Schiøtt B, Vosegaard T, Nielsen NC, Tajkhorshid E (2008) Peptide aggregation and pore formation in a lipid bilayer: a combined coarse-grained and all atom molecular dynamics study. Biophys J 95:4337–4347. doi:10.1529/biophysj.108.133330

Uversky VN, Li J, Souillac P, Millett IS, Doniach S, Jakes R, Goedert M, Fink AL (2002) Biophysical properties of the synucleins and their propensities to fibrillate: inhibition of α-synuclein assembly by β- and γ-synucleins. J Biol Chem 277:11970–11978. doi:10.1074/jbc.M109541200

Valéry C, Artzner F, Paternostre M (2011) Peptide nanotubes: molecular organisations, self-assembly mechanisms and applications. Soft Matter 7:9583–9594. doi:10.1039/C1SM05698K

van der Spoel D, Lindahl E, Hess B, Groenhof G, Mark AE, Berendsen HJC (2005a) GROMACS: fast, flexible and free. J Comput Chem 26:1701–1718. doi:10.1002/jcc.20291

van der Spoel D, Lindahl E, Hess B, Kutzner C, van Buuren AR, Apol E, Meulenhoff PJ, Tieleman DP, Sijbers ALTM, Feenstra KA, van Drunen R, Berendsen HJC (2005b) Gromacs user manual version 4.0. www.gromacs.org

van Gunsteren WF, Berendsen HJC (1988) A leap-frog algorithm for stochastic dynamics. Mol Simul 1:173–185. doi:10.1080/08927028808080941

Vauthey S, Santoso S, Gong H, Watson N, Zhang S (2002) Molecular self-assembly of surfactant-like peptides to form nanotubes and nanovesicles. Proc Natl Acad Sci USA 99:5355–5360. doi:10.1073/pnas.072089599

Velichko YS, Stupp SI, de la Cruz MO (2008) Molecular simulation study of peptide amphiphile self-assembly. J Phys Chem B 112:2326–2334. doi:10.1021/jp074420n

Villa A, Peter C, van der Vegt NFA (2009) Self-assembling dipeptides: conformational sampling in solvent-free coarse-grained simulation. Phys Chem Chem Phys 11:2077–2086. doi:10.1039/B818144F

Walsh DM, Lomakin A, Benedek GB, Condron MM, Teplow DB (1997) Amyloid β-protein fibrillogenesis: detection of a protofibrillar intermediate. J Biol Chem 272:22364–22372. doi:10.1074/jbc.272.35.22364

Walsh DM, Hartley DM, Kusumoto Y, Fezoui Y, Condron MM, Lomakin A, Benedek GB, Selkoe DJ, Teplow DB (1999) Amyloid β-protein fibrillogenesis: structure and biological activity of protofibrillar intermediates. J Biol Chem 274:25945–25952. doi:10.1074/jbc.274.36.25945

Wang J, Tang F, Li F, Lin J, Zhang Y, Du L, Zhao X (2008) The amphiphilic self-assembling peptide EAK16-I as a potential hydrophobic drug carrier. J Nanomater 2008:516286. doi:10.1155/2008/516286

Wen Y, Kolonich HR, Kruszewski KM, Giannoukakis N, Gawalt ES, Meng WS (2013) Retaining antibodies in tumors with a self-assembling injectable system. Mol Pharm 10:1035–1044. doi:10.1021/mp300504z

Wen Y, Liu W, Bagia C, Zhang S, Bai M, Janjic JM, Giannoukakis N, Gawalt ES, Meng WS (2014a) Antibody-functionalized peptidic membranes for neutralization of allogeneic skin antigen-presenting cells. Acta Biomater 10:4759–4767. doi:10.1016/j.actbio.2014.08.003

Wen Y, Roudebush SL, Buckholtz GA, Goehring TR, Giannoukakis N, Gawalt ES, Meng WS (2014b) Coassembly of amphiphilic peptide EAK16-II with histidinylated analogues and implications for functionalization of β-sheet fibrils in vivo. Biomaterials 35:5196–5205. doi:10.1016/j.biomaterials.2014.03.009

Yan Z, Wang J, Wang W (2008) Folding and dimerization of the ionic peptide EAK16-IV. Proteins 72:150–162. doi:10.1002/prot.21903

Yang H, Fung S-Y, Pritzker M, Chen P (2007a) Surface-assisted assembly of an ionic-complementary peptide: controllable growth of nanofibers. J Am Chem Soc 129:12200–12210. doi:10.1021/ja073168u

Yang H, Fung S-Y, Pritzker M, Chen P (2007b) Modification of hydrophilic and hydrophobic surfaces using an ionic complementary peptide. PLoS one 2:e1325. doi:10.1371/journal.pone.0001325

Zhang S, Lockshin C, Herbert A, Winter E, Rich A (1992) Zuotin, a putative Z-DNA binding protein in *Saccharomyces cerevisiae*. EMBO J 11:3787–3796

Zhang S, Yan L, Altman M, Lässle M, Nugent H, Frankel F, Lauffenburger DA, Whitesides GM, Rich A (1999) Biological surface engineering: a simple system for cell pattern formation. Biomaterials 20:1213–1220. doi:10.1039/C2JM31620J

Zhou J, Thorpe IF, Izvekov S, Voth GA (2007) Coarse-grained peptide modeling using a systematic multiscale approach. Biophys J 92:4289–4303. doi:10.1529/biophysj.106.094425